

# Bimodal growth of the nanophases in the dual-phase composites produced by mechanical alloying in immiscible Cu–Ag system

M. Zhu · Z. F. Wu · M. Q. Zeng · L. Z. Ouyang · Y. Gao

Received: 8 October 2007 / Accepted: 7 February 2008 / Published online: 11 March 2008  
© Springer Science+Business Media, LLC 2008

**Abstract** Annealing was carried out to produce Ag–Cu dual-nanophase composite by decomposing Ag–Cu supersaturated solid solution prepared by ball-milling. Differential scanning calorimetry, X-ray diffraction, and transmission electron microscopy were used to characterize the growth kinetics of the nanophase composite upon heating. The results show that bimodal growth kinetics is obeyed in the dual-nanophase system. The coarsening of the second phase of small volume fraction follows the cubic law of LSW theory, while the grain growth of matrix phase follows the kinetic equation of the grain growth of pure nanocrystalline metals. In both cases, the growth is controlled by grain boundary diffusion.

## Introduction

Nanocrystalline materials have attracted both scientific and technical interest owing to their unique properties related to their nanostructure, and the advent of many new theoretical problems [1, 2]. Owing to the very high volume ratio of boundary region, nanocrystalline alloys possess inherently a very high interfacial energy which provides a strong driving force for grain growth. Therefore, the stability of nanocrystalline alloys plays a key role in both their properties and structure.

As it is well known, the isothermal grain growth of highly pure metals with conventional grain size is usually represented by the following equation [3]:

$$R^n - R_0^n = kt \quad (1)$$

where,  $R$  is the mean grain size at annealing time  $t$ ,  $k$  is a constant that depends on temperature,  $R_0$  is the initial mean grain size and  $n$  is an empirical constant usually taking the value within a range of 0.25–0.5. By considering the grain growth process associated with the pinning effect of grain boundaries by second-phase particles, impurities, pores or surfaces in metals with low impurity and/or alloying solutes, Burke obtained an equation for isothermal grain growth kinetics of metals with low impurity and/or alloying solutes by assuming the drag force caused by boundary pinning to be independent of conventional grain size [3].

Experimental results indicate, however, that the grain growth kinetics in nanocrystalline metals can rarely be described by Eq. 1 or Burke equation. The mechanism controlling growth kinetics is affected by various microstructure features such as initial grain size [4], grain boundary feature [5], solute drag [6], and internal strains [7]. Michels [8] modified the Burke model by considering the retarding force on grain boundary migration to be dependent on grain size and obtained the following grain growth equation:

$$\frac{R^2 - R_{\max}^2}{R_0^2 - R_{\max}^2} = \exp\left(-\frac{2kt}{R_{\max}^2}\right) \quad (2)$$

The rate constant  $k$  can be expressed in an Arrhenius type equation:

$$k = k_0 \exp\left(-\frac{Q}{R_B T}\right) \quad (3)$$

where  $Q$  is activation energy for isothermal grain growth,  $R_B$  is universal gas constant ( $8.31 \text{ J mol}^{-1} \text{ K}^{-1}$ ), and  $k_0$  is a constant independent of the absolute temperature  $T$ . The activation energy  $Q$  is often used to characterize the

M. Zhu (✉) · Z. F. Wu · M. Q. Zeng · L. Z. Ouyang · Y. Gao  
School of Mechanical Engineering, South China University  
of Technology, Guangzhou 510640, China  
e-mail: memzhu@scut.edu.cn

mechanism dominating grain growth. In fact, the grain growth behavior of nanocrystalline metals is quite complicated. Abnormal growth was often observed in the initial stage of grain growth and it has been considered to be related to impurity segregation in grain boundary [4, 9]. The grain growth at high and low annealing temperature was governed by lattice diffusion and grain diffusion, respectively [9, 10]. This may be due to the fact that the grain size of high temperature annealed sample is bigger. It has also been found that alloying addition and stress have apparent effect on grain growth of nanocrystalline metals. For instance, the addition of Co increases the thermal stability of nanocrystalline Ni [11], and tensile plastic deformation results in grain growth in nanocrystalline alloys [12, 13].

Nanophase composite alloys, which consist of at least two phases in nanometer size, have potential application in the fields of magnetic materials [14], hydrogen storage materials [15], hard metals [16], and so on. The thermal stability of nanophase composite alloys is also very important and of great interest [17, 18]. For the conventional grain sized alloys, the self-similar coarsening of dispersed particles embedded in a matrix with very small volume fraction, also known as Ostwald ripening, is generally described by Lifshitz–Slyozov–Wagner (LSW) theory [19, 20]. Effort has been made to modify LSW theory and extend it to high volume fraction of dispersed phases using both analytic and numerical methods [21, 22]. The results show that the growth law of LSW theory can be used for embedded phase of high volume fraction, with the coarsening rate being dependent on volume fraction.

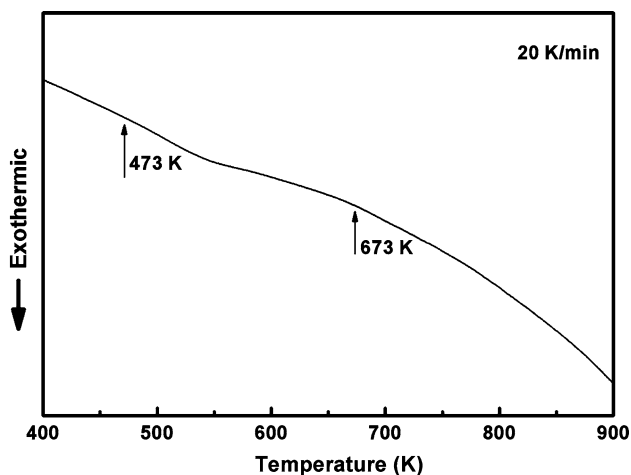
For the nanophase composite alloys, research has been focused mainly on the coarsening of secondary phases of small volume fraction and the results show that the activation energy for the grain growth of nanophase composites is different from that of conventional grain sized alloys although the cubic law of LSW theory is still applicable [17, 18]. It is therefore of significance to investigate the mechanism of Ostwald ripening behavior of nanophase composite alloys in more details. On the other hand, the growth behavior of the matrix phase in nanophase composite alloys should be also deeply revealed to have a comprehensive understanding of their thermal stability. The purpose of the present work is to investigate the growth behavior of both matrix and secondary phase in nanophase composites and to understand the mechanism of grain growth in more details. Cu–Ag system was selected for the reason that the volume ratio of Ag phase to Cu phase keeps constant in the growing process even at quite high temperature due to the immiscibility of the system and it is a system that has important application as electric contact materials.

## Experimental

Cu and Ag powders of 99.9% purity and 200-mesh size were used as raw materials. The powder mixtures of Cu–20at.%Ag and Cu–80at.%Ag were hermetically sealed in stainless steel vials together with hardened steel balls and milled in a Fritsch P5 planetary ball mill. The weight ratio of the powder to ball was 1:15. The handling of powders and milling process were performed under the protection of pure argon gas. Differential scanning calorimetry (DSC) measurement was made to determine the decomposition temperature on a PE DSC 7 at a scanning rate of 20 K/min. The milled powders were heated at different temperatures for different dwelling times under the protection of pure argon gas. A Philips X'pert MPD Pro X-ray diffractometer (XRD) with Cu  $K_{\alpha}$  radiation and a JEOL2010 transmission electron microscopy (TEM) were used to characterize the microstructure evolution of the alloys treated by different heating processes. Samples for TEM observation were prepared by dispersing the powders onto a grid covered by carbon. The average grain sizes of Cu and Ag phases were estimated from the peak broadening of X-ray diffraction peaks by the Vogit method [23].

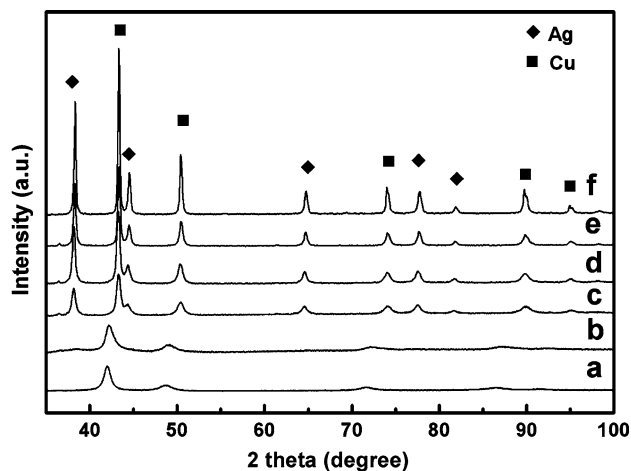
## Experimental results

In order to obtain a dual-nanophase composite consisting of matrix and secondary phase, alloys with composition of Cu–20at%Ag and Cu–80at%Ag were selected. In the former alloy, the volume fraction of Cu and Ag phase is 73.4% and 26.6%, respectively, and Cu and Ag are hence regarded as matrix phase and secondary phase, respectively. In the latter one, the volume fraction of Cu and Ag phase is 14.7% and 85.3%, respectively, and Cu and Ag are hence, regarded as secondary phase and matrix phase, respectively. It has been proved that nanocrystalline supersaturated solid solution can be obtained in this system by mechanical alloying (MA) [24]. Therefore, nanophase composite of Ag and Cu phase can be obtained by heating to decompose the supersaturated solid solution. In order to avoid the correlative effect of decomposition and growth processes of nanophases, it is necessary to study the growth behavior of the alloy which has completed the decomposition process. Thus, DSC and XRD analysis were employed to characterize the decomposition of supersaturated solid solution. Figure 1 shows the DSC heating scan curve of Cu–20%Ag sample milled for 30 h. The DSC trace shows a single exothermic peak in a temperature range of 473–673 K. In order to reveal the origin of the exothermic event, the as milled powders were heated in the DSC to different temperatures at a heating rate of 20 K/min, and then rapidly cooled at rate of 50 K/min. The



**Fig. 1** DSC heating scan curve of Cu–20%Ag alloy after 30 h of milling, heating rate 20 K/min

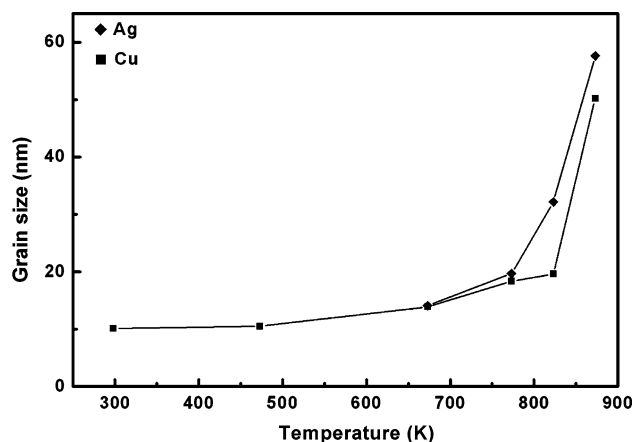
treated samples were characterized by XRD analysis. Figure 2 shows the X-ray diffractograms of Cu–20%Ag alloy samples heated at 473, 673, 773, 823, and 873 K. The diffractogram of the as-milled sample was also put in Fig. 2 for comparison. As shown in Fig. 2a, the diffraction peaks of Ag disappear completely after milling and there remain only the diffraction peaks of Cu which have significantly shifted toward lower angles, indicating an increase of lattice constant due to the dissolving of Ag into Cu, owing that the atomic radius of Ag (0.144 nm) is larger than that of Cu (0.128 nm). The diffraction peaks of Cu broaden apparently in the as-milled sample, which indicates the substantial refinement of its grain size and existence of internal strain caused by milling. As estimated from the broadening of diffraction peaks, the average grain size of Cu phase is about 10 nm.



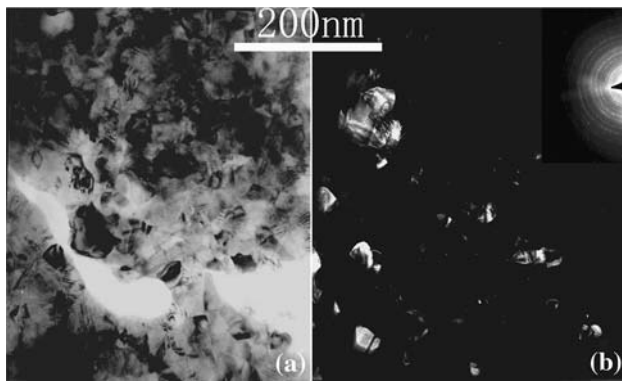
**Fig. 2** X-ray diffractograms of Cu–20%Ag alloy heated at different temperatures after 30 h of milling: (a) as-milled; (b) 473 K; (c) 673 K; (d) 773 K, (e) 823 K, and (f) 873 K

Figure 2b and c show the X-ray diffractograms of Cu–20%Ag alloys heated to 473 and 673 K, respectively, after 30 h of milling. As Fig. 2b reveals, the diffraction peaks of Cu significantly shift toward higher angles, indicating that Ag solutes dissolved in Cu begin to precipitate by heating to 473 K (onset point of exothermic peak). For the sample heated to 673 K (ending point of exothermic peak), the diffraction peaks of Ag phase appear in the X-ray diffractogram in Fig. 2c and the positions of Cu peaks almost coincide with those of un-milled Cu powders, which means that Ag atoms dissolved in Cu almost completely precipitated. Thus, by heating to 673 K the nanocrystalline supersaturated solid solution Cu (Ag) alloy was decomposed to nanophase composite of Ag and Cu. Based on this result, the Cu–20%Ag sample heated to 673 K was taken as the initial state for the phase coarsening studying of the Cu–Ag nanophase composite. As estimated from the diffraction peak broadening, the average grain sizes of both Cu and Ag phase are about 14 nm in the sample heated to 673 K. It can be seen that no obvious grain growth of nanophase Cu occurred at this stage. Therefore the exothermic peak on the DSC curves basically aroused from the precipitation of the solute atoms Ag. The diffraction peaks of both Cu and Ag phases become narrow upon further heating, as shown in Fig. 2d–f, which indicates an apparent grain growth of both Cu and Ag phases. Figure 3 gives the dependence of average grain size of Cu and Ag phases on heating temperature, which shows that the grain size of Cu and Ag phases increases obviously with the increase of heating temperature when the temperature is higher than 773 K.

Figure 4a and b are bright and dark field TEM morphology images, respectively, of Cu–20%Ag alloy prepared by heating the milled powders at 873 K for 1 h. The grain size of Cu and Ag phases in Fig. 4 are in good agreement with that obtained by XRD analysis. It has also



**Fig. 3** Dependence of the grain size of Ag and Cu on heating temperature for Cu–20%Ag alloy after 30 h of milling



**Fig. 4** TEM images of Cu–20%Ag alloy heating at 873 K for 1 h after 30 h of milling. (a) Bright field image and (b) dark field image taken by using a section of (111) diffraction ring of Ag

been noted from the TEM images that the phase of small volume fraction distributes homogeneous and most particles are single crystal. Therefore, it is assumed that the grain size of small volume fraction phase represents its particles size in the nanophase composite.

In order to clarify the growth kinetics of Ag nanophase, the dependence of Ag particle size, which was deduced from X-ray diffraction analysis, on heating dwelling time was determined and illustrated in Fig. 5. It is clear that there exists an excellent linear relationship between the cubic of particle size ( $r$ ) and dwelling time ( $t$ ) in the particle size range in this work. Here,  $r_0$ , 7 nm, is the radius of the Ag particles in the initial state of coarsening obtained by annealing at 673 K as mentioned before. Moreover, it is worth mentioning that other power-law dependences, such as  $r^2$  and  $r^4$ , do not yield a satisfactory fitting to the experimental data. The excellent linear relationship between the cubic of  $r$  and  $t$  is just what the so-called

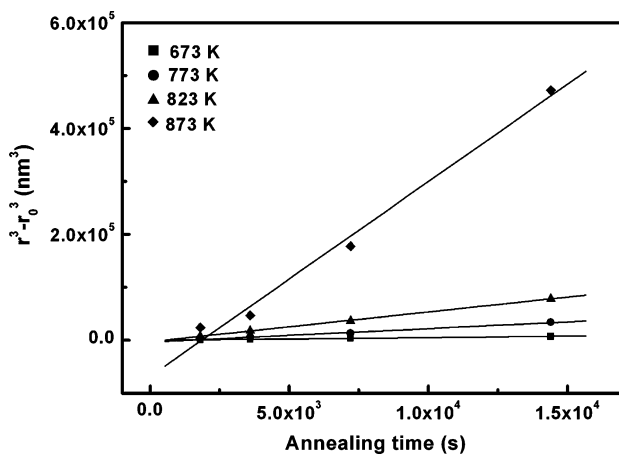


**Fig. 5** Dependence of the cubic of Ag particle radius on heating time for Cu–20%Ag alloy heated at different temperatures (673, 773, 823 and 873 K) after 30 h of milling

classical theory of Ostwald ripening described by LSW equation as given below:

$$r^3 - r_0^3 = Kt \quad (4)$$

where

$$K = \frac{8D\gamma c_\infty V_m^2}{9R_B T} \quad (5)$$

Here,  $K$  is coarsening rate, which can be obtained from the slope of the straight lines correlated between the cubic  $r$  and  $t$ , like those in Fig. 5,  $D$  is volume diffusion coefficient of a solute in a solvent,  $\gamma$  is the interfacial energy between Ag and Cu phases,  $c_\infty$  is the solubility of Ag in Cu solid-solution. Our experimental results on the coarsening of the Ag nanophase particles are in excellent agreement with the LSW theory in the size range of 14–160 nm. This suggests that the classical LSW cubic law can be applied to dual-nanophase composite.

By analyzing the coarsening rate  $K$ , further details related to coarsening mechanism can be revealed. The volume diffusion coefficient  $D$  for solute atoms (Ag) in a solvent matrix (Cu) in polycrystalline materials can be obtained from the Ref. [25]. However,  $D$  in nanophase composite alloys may be different from that in conventional polycrystalline materials due to the large amount of grain boundaries and phase boundaries which strongly enhance diffusion process. In order to estimate the  $D$  in the Cu–20%Ag nanophase composite, we calculated the interfacial energy ( $\gamma$ ) of Ag/Cu interfaces by Miedema model [26] and got the solubility of Ag in Cu solid-solution at different temperatures (673, 773, 823, and 873 K) according to the Ref. [27].  $D$  is thus obtained according to Eq. 5. In general,  $D$  observes Arrhenius relation with temperature, i.e.,

$$D = D_0 \exp\left(-\frac{Q}{R_B T}\right) \quad (6)$$

where,  $D_0$  is pre-exponential factor and  $Q$  is activation energy of diffusion. At temperatures from 673 to 873 K, a liner relationship exists between  $\ln D$  and  $\frac{1}{T}$ , as shown in Fig. 6. From its slope, an activation energy of 106 kJ/mol for the volume diffusion of Ag coarsening in Cu was obtained for the Cu–20at.%Ag nanophase composite. For comparison, the diffusion activation energy of Ag in Cu of different diffusion mechanisms is given in Table 1. It shows that the value obtained in this work is much smaller than that of lattice diffusion mechanism of Ag in Cu and lattice self-diffusion of Cu but very close to that of boundary self-diffusion of Cu. This reveals the growth mechanism of Ag phase in Cu matrix in nanophase composite Cu–20%Ag alloys and will be discussed later.

The above results describe the coarsening behavior of the Ag phase particle with small volume fraction in Cu–

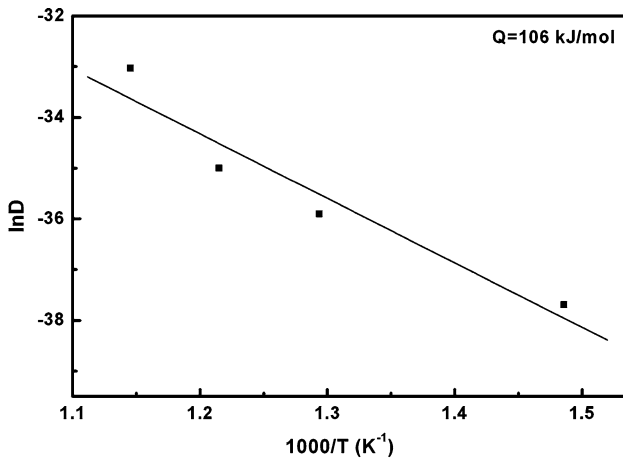


**Fig. 6** Arrhenius plot of diffusion coefficient  $D$  for Ag diffusion in Cu in the ripening process.  $D$  was deduced from  $K$  obtained by experiment

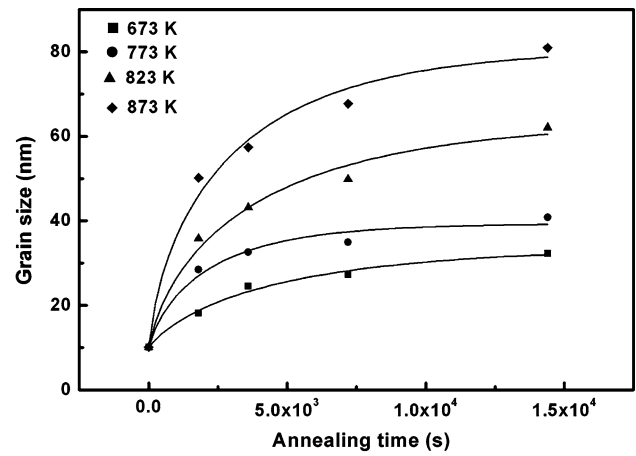


**Fig. 7** Dependence of the grain size of Cu on heating time for Cu–20%Ag alloy heated at different temperatures (673, 773, 823, and 873 K) after 30 h of milling

20%Ag nanophase composite. Now, we are going to describe the coarsening behavior of the matrix phase Cu in the same composite. The average grain sizes of matrix phase Cu as a function of annealing time at different temperatures are shown in Fig. 7. Grain growth stagnates after certain annealing time for all annealing temperatures. At each temperature, the data of grain sizes were fitted to Eq. 2 by using a nonlinear curve fitting computer program to determine the best fitted values for parameters  $k$  and  $R_{max}$ . The solid lines in Fig. 7 are the fitted curves. The measured grain sizes at all temperatures are well fitted by Eq. 2, as can be seen in Fig. 7, and the best fitted values for parameters  $k$  and  $R_{max}$  obtained by this routine are listed in Table 2. The activation energy  $Q$  can be subsequently obtained from the slope of a plot of  $\ln k$  against  $1/T$  as shown in Fig. 8. The overall data in Fig. 8 fit excellently to a straight line. Thus, an activation energy of 46 kJ/mol for the grain growth of matrix phase Cu was obtained. This value is much smaller than the activation energy of lattice self-diffusion of Cu.

**Table 2** Parameters obtained by fitting Eq. 3 to the measured data points in Fig. 7

Heating temperature, $T$ (K)	673	773	823	873
Rate constant, $k$ (nm <sup>2</sup> /s)	0.087	0.245	0.332	0.693
$R_{max}$ (nm)	33.8	39.3	63.4	80.6

In order to understand in more details the growth behavior of the nanophase composite in Ag–Cu system, nanophase composite Cu–80%Ag alloy was also prepared, in which the matrix and the phase of small volume fraction

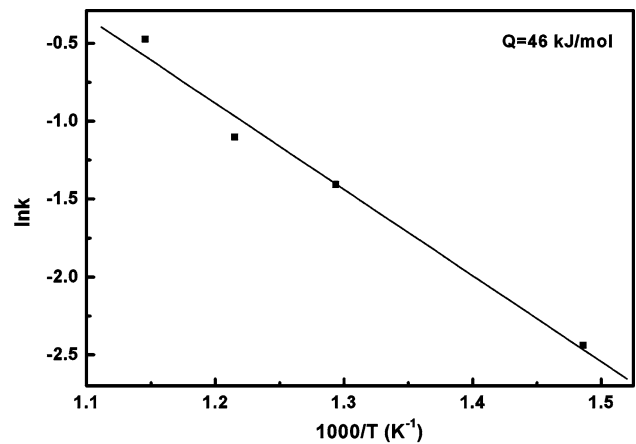


**Fig. 8** Arrhenius plot of the rate constant  $k$  for the growth of matrix phase Cu

**Table 1** Activation energy in kJ/mol of experiment and theory in Ag–Cu system

Alloy systems	Activation energy of our results	Activation energy of lattice diffusion [25]	Activation energy of lattice (self-) diffusion [25]	Activation energy of grain boundary (self-) diffusion [25]
Ag–80%Cu	Ag:106	Ag in Cu	Ag:171.1 (550–1228 K)	Ag:86 (550–1228 K)
	Cu:46	194.7 (873–1273 K)	226.7 (550–1228 K)	113 (550–1228 K)
Ag–20%Cu	Cu:61	Cu in Ag	Cu:197.8 (573–1334 K)	Cu:99 (573–1334 K)
	Ag:55	164.1 (699–897 K)	237.4 (573–1334 K)	118 (573–1334 K)
		193 (990–1218 K)		

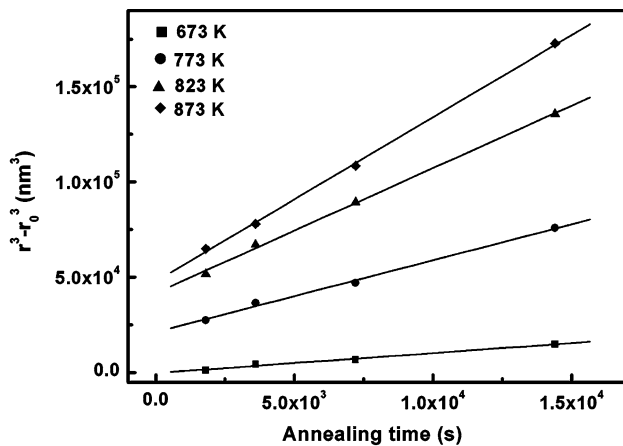


**Fig. 9** Dependence of the cubic of Cu particle radius on heating time for Cu–80%Ag alloy heated at different temperatures (673, 773, 823 and 873 K) after 30 h of milling

is just opposite to the above Cu–20%Ag alloy, and the coarsening behavior of its phases was investigated. Figure 9 shows the growth curves of small volume fraction phase Cu, in Cu–80%Ag alloy at 673, 773, 823, and 873 K for different times. Similar to the growth of Ag phase, being small volume fraction phase in Cu–20%Ag alloy, a good linearity between  $(r^3 - r_0^3)$  and annealing time  $t$  was observed in the growth of small volume fraction phase Cu in Cu–80%Ag alloy, which suggests an excellent agreement with the LSW theory. On the other hand, the growth kinetics of matrix phase, Ag, can also be fitted by Eq. 2, as shown in Fig. 10. Using the same method as described before, the activation energy for the growth of Cu phase and Ag matrix phase was obtained. The obtained results are 61 and 55 kJ/mol for Cu and Ag phase, respectively.

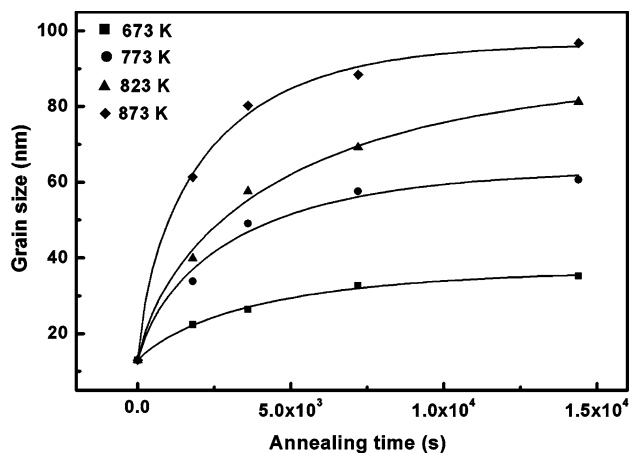


**Fig. 10** Dependence of the particle size of Cu on heating time for Cu–80%Ag alloy heated at different temperatures (673, 773, 823 and 873 K) after 30 h of milling

## Discussions

### Growth mechanism in nanophase composites

The coarsening of the phase with small volume fraction, either Cu or Ag, in Ag–Cu nanophase composite alloys, can be described by the LSW theory, while the growth of matrix phase satisfies the kinetic equation describing the grain growth of pure nanocrystalline metals. The mechanism governing the coarsening of nanophases can be revealed to some extent by comparing the obtained activation energy of the growth of each nanophase with the activation energy in different diffusion mechanisms in conventional Cu–Ag alloys as listed in Table 1. It is noted that the activation energies of grain boundary self-diffusion for Cu and Ag were reported different in different references. In the present work, we choose the values of 99 and 86 kJ/mol as the grain boundary self-diffusion activation energies for Cu and Ag, respectively, as most researches did. Considering the data in Table 1, the growth activation energies of the phases with small volume fraction in Cu–Ag alloys, 106 kJ/mol for Ag, and 61 kJ/mol for Cu, are obviously lower than that of lattice diffusion for solute atoms in solvent matrix in conventional polycrystalline alloys, but close to the activation energy of grain boundary self-diffusion of solvent matrix, 99 kJ/mol for Cu and 86 kJ/mol for Ag. This result indicates that the ripening mechanism in the nanophase composite alloys is different from that in conventional dual-phase systems. The observation of the cubic law for the coarsening of the phases with small volume fraction in the nanophase composite alloys reveals that the ripening process is controlled by the three-dimensional long distance diffusion of solute atoms. However, the agreement of the activation energy to that of grain boundary self-diffusion of matrix indicates that the diffusion mechanism in the nanophase composite alloys is basically grain boundary diffusion. This is because the grain sizes of matrix phase and the phase with small volume fraction are all in nanometer range, less than 160 nm for Ag–80%Cu and Ag–20%Cu. Thus, the solute atoms should diffuse more easily along nanograin boundary than in conventional dual-phase systems, as demonstrated in Fig. 11.

The growth of matrix phase in Ag–Cu nanophase composite alloys follows the kinetic equation describing the grain growth of pure nanocrystalline metals. However, the activation energies, 46 kJ/mol for Cu and 55 kJ/mol for Ag, are not only smaller than those of the lattice self-diffusion of Cu and Ag, but also significantly smaller than those of grain boundary self-diffusion in conventional polycrystalline alloys. This is mainly due to the high volume fraction of grain boundaries/interfaces in nanophase composite alloys and the growth of matrix phase is

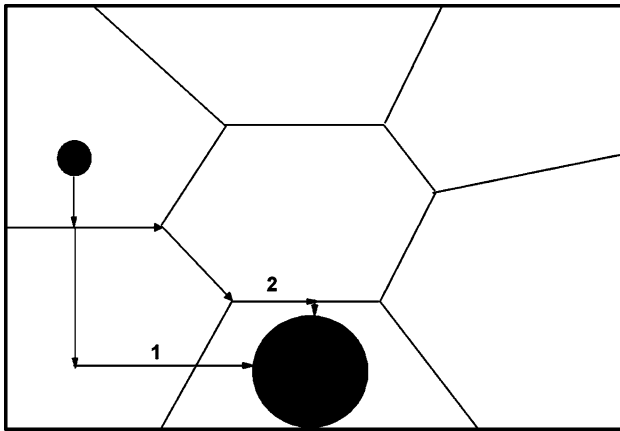


**Fig. 11** Two diffusion mechanisms of solute atoms during Ostwald ripening. The second route is preferential for nanophase composites

controlled by nanograin boundary diffusion. As it has been reported [28], the activation energy for the growth of pure nanocrystalline Cu is  $30 \pm 9$  kJ/mol which is only about one third of the activation energy of grain boundary diffusion in polycrystalline Cu.

Based on the above considerations, it is found that there exist two different growth mechanisms, bimodal growth mechanism, in nanophase composite alloys. For the matrix phase, the growth kinetics is similar to that of pure nanocrystalline metal with the grains growing via grain boundary migration controlled by grain boundary diffusion. For the phase with small volume fraction, the growth kinetics satisfies the classical LSW theory for the coarsening of secondary phase and the coarsening is a long distance volume diffusion controlled by grain boundary diffusion.

#### Activation energy for grain boundary inter-diffusion

Considering the growing process described above, the activation energy of inter-diffusion can be estimated. For the coarsening of Ag in Cu–20%Ag system, the diffusion of Ag is primarily along the grain boundaries of Cu matrix. Thus, the activation energy obtained is the diffusion activation energy of Ag in Cu. In this case, the diffusion of solute atoms (Ag) along the grain boundaries of the solvent matrix (Cu) is more difficult than the grain boundary self-diffusion because the atom radius of Ag is larger than that of Cu. Thus the growth activation energy (106 kJ/mol) of Ag, as a secondary phase, is larger than that of the grain boundary self-diffusion of Cu (99 kJ/mol). Similarly, the growth activation energy (61 kJ/mol) of Cu as a secondary phase is smaller than that of the grain boundary self-diffusion of Ag (86 kJ/mol) because the diffusion of solute atoms (Cu) along the grain boundaries of solvent matrix (Ag) is easier than the grain boundary self-diffusion of Cu.

According to the above discussion, we can measure inter-diffusion activation energy along grain boundary in immiscible system by characterizing the coarsening of their nanophase composites. This gives us a possibility of measuring the activation energy of grain boundary inter-diffusion of immiscible systems which is not easy to measure experimentally.

#### Summary

The growth kinetics of nanophase composites in immiscible Cu–Ag system produced by annealing mechanically alloyed supersaturated solid solution was investigated. It has been proved that a bimodal growth takes place in the nanophase composite alloys. For the matrix phase, the growth kinetics can be well described by the equation proposed for nanocrystalline pure metals and the growing is grain boundary migration controlled by grain boundary diffusion. For the coarsening of the secondary phase with small volume fraction, the ripening process satisfies the cubic law of classical LSW theory and the coarsening is a long distance volume diffusion controlled by grain boundary diffusion. The present experiment results suggest that the activation energy of grain boundary inter-diffusion can be revealed by analyzing the growth kinetics of small volume fraction phase in nanophase composites.

**Acknowledgements** The financial supports from Ministry of Education of China (IRT 0551) and Guangdong Provincial Natural Science Foundation (Team Project) are greatly acknowledged.

#### References

1. Padmanabhan KA (2001) *Mater Sci Eng A* 304–306:200
2. Gleiter H (2000) *Acta Mater* 48:1
3. Humphrey FJ, Hatherly M (1996) *Recrystallization and related annealing phenomena*, 1st ed. Pergamon Press, Oxford, England, Oxford, p 253
4. Hibbard GD, McCrea JL, Pzumbo G, Aust KT, Erb U (2002) *Scripta Mater* 47:83
5. Qian LH, Wang SC, Zhao YH, Lu K (2002) *Acta Mater* 50:3425
6. Knauth P, Charai A, Gas P (1993) *Scripta Metall et Mater* 28:325
7. Liu KW, Mucklich F (2001) *Acta Mater* 49:395
8. Michels A, Krill CE, Ehrhardt H, Birringer R, Wu DT (1999) *Acta Mater* 47:2143
9. Ebrahimi F, Li H (2006) *Scr Mater* 55:263
10. Jonkowski AF, Saw CK, Hayes JP (2006) *Thin Solid Films* 515:1152
11. Hibbard GD, Aust KT, Erb U (2006) *Mater Sci Eng A* 433:195
12. Fan GJ, Fu LF, Choo H, Liaw PK, Browning ND (2006) *Acta Mater* 54:4781
13. Li JCM (2006) *Phys Rev Lett* 96:215506
14. Betancourt JI, Davies HA (2002) *J Magn Magn Mater* 246:6
15. Zhu M, Wang H, Ouyang LZ, Zeng MQ (2006) *Int J Hydrogen Energy* 31:251

16. Cha SI, Hong SH, Ha GK, Kim BK (2001) *Int J Refrac Metals Hard Mater* 19:397
17. Yu JH, Kim TH, Lee JS (1997) *NanoStruct Mater* 9:229
18. Wu ZF, Zeng MQ, Ouyang LZ, Zhang XP, Zhu M (2005) *Scripta Mater* 53:529
19. Lifshitz IM, Slyozov VV (1961) *J Phys Chem Solids* 19:35
20. Wagner C (1961) *Phys Chem* 65:581
21. Voorhees PW, Glicksman ME (1984) *Acta Metall* 32:2001
22. Enomoto Y, Tokuyama M, Kawasaaki K (1986) *Acta Metall* 34:2119
23. Langford JL (1978) *J Appl Cryst* 11:10
24. Uenishi K, Kobayashi KT, Ishihara KN, Shingu PH (1991) *Mater Sci Eng A* 134:1342
25. Gale WE, Totemeier TC (2004) *Smithells materials reference book*, 8th ed. Elsevier, Butterworth-Heinemann, pp 13–10, 13–16, 13–19
26. Miedema AR, Den Broeder FJA (1979) *Z Metallkde* 70:14
27. Ma E, He JH, Schilling PL (1997) *Phys Rev E* 55:5542
28. Ganapathi SK, Owen DM, Choksh AH (1991) *Scripta Metall et Mater* 25:2699